Progress In Electromagnetics Research, PIER 64, 239–255, 2006

MIXED FAULT DIAGNOSIS IN THREE-PHASE SQUIRREL-CAGE INDUCTION MOTOR USING ANALYSIS OF AIR-GAP MAGNETIC FIELD

J. Faiz

Department of Electrical and Computer Engineering
Campus No. 2
Faculty of Engineering
University of Tehran
North Kargar Avenue, Tehran, 1439957131, Iran

B. M. Ebrahimi

Department of Electrical and Computer Engineering
University of Tabriz
Tabriz, Iran

Abstract—In this paper fault diagnosis of induction motor under mixed fault is carried out using precise analysis of the air-gap magnetic field based on time stepping finite element method. By feeding voltage instead of current density to the finite element computation part, the drawbacks of the application of finite element method in fault diagnosis of induction motor are overcome. Normally static eccentricity and broken rotor bars faults have been individually diagnosed in the published papers. Here diagnosis of the mixed fault, including static eccentricity and broken rotor bars, is introduced which is considered as a novel part of the present work. Precise analysis of magnetic field in the air-gap of a faulty induction motor is carried and performance of the motor is predicted. Taking into account the magnetic core saturation is another advantage of the present work. This is required in the transient analysis of a faulty motor.

1. INTRODUCTION

Fault diagnosis systems are used as a tool for maintenance and protection of the costly systems against faults. These systems predict performance by receiving the required information from the system or

process. If the predicted performance corresponds with the defined fault conditions, the relevant fault is flagged. The most important benefit of fault diagnosis is that the probable damage of system can be predicted by analysis of parameters changes. Even it is possible to estimate the fault instant and specify the part that causes such fault [1].

Magnetic field distribution within the motor contains full information on the stator, rotor and mechanical parts of the motor [2]. Having this magnetic field distribution makes it possible to evaluate the actual performance of the motor. Therefore, all electrical motors faults can be diagnosed by continuous analysis of the magnetic fields [2]. Abnormal magnetic field distribution as the results of the broken rotor bars and eccentricity degrades the steady-state and dynamic performance of the motor. Changes of parameters of the motor caused by different faults are taken into account and, the performance of the motor is then predicted.

In practice, the air gap magnetic field can be measured by a small search coil where a sensor is fixed in the air gap and the noise effect upon the sent signals is eliminated. In [3], it has been shown that the fault can be detected by a search coil outside the machine. Generally, there are three major methods for modeling, analysis and diagnosis of faults in induction motor: winding function method (WFM), equivalent magnetic circuit method (MECM) and finite element method (FEM).

The WFM normally ignores the core saturation [4–10]. Basically the WFM cannot easily take into account the magnetic field saturation effect upon the performance of the motor. Therefore, continuous inspection of the magnetic field for fault analysis and diagnosis is impossible using the WFM. The MECM needs shorter computation time compared with the FEM, but it is less accurate. Meanwhile, the directions of the magnetic flux lines must be already known [11]. It is noted that the precise mathematical models of the motor are complicated and methods such as the MECM or *d-q-o* model is not capable to diagnose the fault in the real cases [12, 13]. FEM is based on the magnetic field analysis that is capable to include spatial harmonics effects due to the topology of magnetic circuits, split winding pattern, non-linearity of ferromagnetic material and different faults in the stator and motor [14–19]. Magnetic field distribution within the motor can be evaluated using FEM, based on the dimensions and magnetic parameters of the motor. Knowing the magnetic field distribution, other quantities, such as induced voltage waveform, magnetic flux density within the air gap and inductances of different windings of the motor are obtained [20–23].

In [2], magnetic field and flux density have been obtained for a motor with 3 and 4 broken bars. It has been shown that the location of rotor bar breakage influence the magnetic field distribution. In [3], magnetic field distribution within a healthy machine and a machine with 5 broken bars are obtained. Also it has been shown that the broken rotor bars can be detected by inserting a number of few search coils inside and outside of the machine. It has been proved that only a search coil outside machine can diagnose the rotor bars breakage. In [1, 3], the current of the broken bars is taken to be zero which means a considerable increase of the adjacent bars current. However, by taking into account the inter-bar current, the above assumption is not so valid. The next point is that, in the above-mentioned paper only broken rotor bars have been investigated while presence of intrinsic static eccentricity, existing even in new motors, must be taken into account [24]. In other words mixedfault must be considered. The last point is that in the FEM, current density is taken to be the input. If the object is not determination of the current frequency spectrum or analyzing transient mode, such assumption can be applied. Otherwise, the motor winding current must be calculated using alterative method, and this may complicate the FEM application [1].

Time stepping finite element coupled state-space (TSFE-SS) method can be used to calculate the inductances of the machine, current and other required variables are then determined by an analytical method, and they are used as input of the FE equations. This iterative process continues up to converging the actual solution. It is necessary to emphasize that this convergence depends on the initial values of the current and rotor angular position. Also, FEM has been only used for inductance estimation, the remaining computations and analyses have been carried out in the space state, it means that two different procedures must be employed which complicated the computations process.

This paper does not assume a zero current for broken rotor bars but the resistance of such rotor bar is taken to be large. In this paper, the TSFE technique is used for analysis and diagnosis of a mixed fault in induction motor where voltage supply considered as input of FE computation part. Then stator phase current is calculated as the unknown value. Since all calculations and analyses are carried using FEM, a very high precision is achieved.

So far FEM methods have been used for analysis and diagnosis of fault in induction motor in the steady-state case, while noise, unbalanced magnetic pull (UMP) and even arcing occur during the starting mode. Therefore, in the present paper electromagnetic torque of the healthy motor, motor with static eccentricity and motor with

mixed fault during the starting period are analyzed. In addition, in the proposed modeling, geometrical complexities of the stator structure and rotor, spatial distribution of the stator windings, slots on both sides of the air gap and non-linearity of the core materials are taken into account. The drive elements of the motor are paid a special attention because the magnetic forces somehow determine the positions of these elements and these positions in turn affect the internal magnetic field of the motor. Since there is inter-bar current in broken rotor bars, the broken bars current in the modeling relevant to the breakage of the bars, is not assumed equal to zero, but the resistance of the broken bar is considered a large value. In the introduced FEM the input of the FE equations is voltage.

Magnetic flux and flux density for a healthy motor, a motor with 1 broken rotor bar and 10% static eccentricity and 4 broken rotor bars and 30% static eccentricity are studied. The results are presented for a three-phase, 4 poles, 230 V, 3 hp and 60 Hz induction motor. Opera 20–10.5 package is used for FE computations.

2. BROKEN ROTOR BAR, STATIC ECCENTRICITY, AND MIXED-FAULT

2.1. Broken Rotor Bars

The reason for around 5 to 10% of the faults in squirrel-cage induction motors is broken rotor or cracked bars and end-rings breakage [30]. There are many reasons for such faults which include: thermal stress due to over load, non-uniform heat distribution, hot spot and arc, magnetic stresses due to the electromagnetic force, unsymmetrical magnetic force, electromagnetic vibrations, residual stress from manufacturing stage, dynamic stress due to axial torque, environmental stress due to the contamination, materials wearing by chemical materials and humidity mechanical stress due to mechanical fatigue of different parts, faulty ball-bearings and laminations loosing [31]. Fig. 1 presents a distributed model of squirrel-cage rotor of a healthy motor. As shown in this figures, every two adjacent bars form a loop. Fig. 2 presents the distributed model of a squirrel-cage rotor with a broken rotor bar.

2.2. Static Eccentricity

When the rotor, stator and rotational axes of a motor are not coincide, the air gap becomes non-uniform. Approximately 80% of the mechanical faults lead to the stator and rotor eccentricity [32]. Of course, this eccentricity may occur during the process of manufacturing

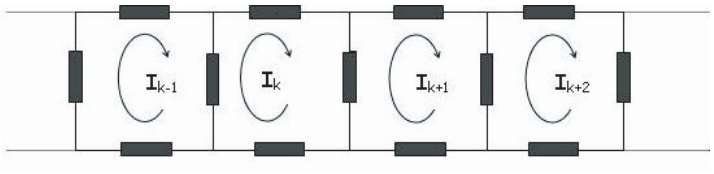

Figure 1. Distributed form of rotor cage for a healthy motor.

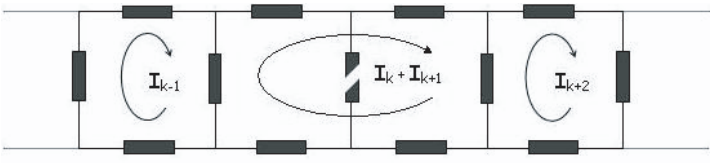

Figure 2. Distributed form of rotor cage for a motor with one rotor broken bar.

and fixing the rotor. There is different eccentricity including static, dynamic and mixed. When the static eccentricity occurs, the rotor rotational axe is coincide with its symmetry axe, but has displacement with the stator symmetrical axe. In this case, the air gap around the rotor misses its uniformity, but it is invariant with time. Fig. 3 shows the cross section of the proposed induction motor and Fig. 4 exhibits the corresponding figure with static eccentricity.

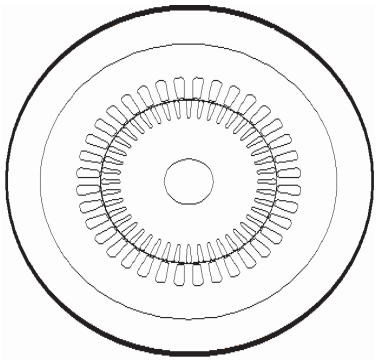

Figure 3. Cross-section of proposed induction motor.

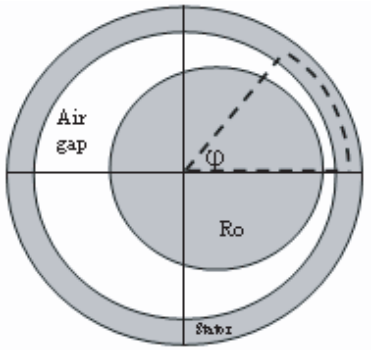

Figure 4. Cross-section of stator and rotor positions with static eccentricity.

2.3. Mixed-Faults

In the case of broken rotor bars in the presence of the intrinsic static eccentricity, the instantaneous presence of two faults must be considered. Meanwhile, rotor bars breakage causes the static eccentricity and it is possible that two faults occur simultaneously.

3. FE ANALYSIS OF INDUCTION MOTOR UNDER FAULT

Previously FE was applied for steady-state analysis of electrical machine, but now it can be easily used for transient analysis due to the availability of more powerful computers. However, solving the governing equations of FEM needs long computation time. It is possible to reduce the computation time by using the geometrical symmetry of the machine. For example, one quarter of machine can be considered and the obtained magnetic field is extended for the whole structure of the machine. However, this cannot be used for mixed fault induction motor, because there is no symmetry any more.

Both healthy and faulty induction motors are modeled as shown in Fig. 5. In the modeling of the faulty induction motor the terminal voltage is applied to the motor as the known input value.

The outer circuit showing the electric sources and unknown circuit elements must be combined with the field equation of FE technique [19] in order to form the transient equations. The non-linear equation enabling to relate the FE formula (expressing electromagnetic fields of

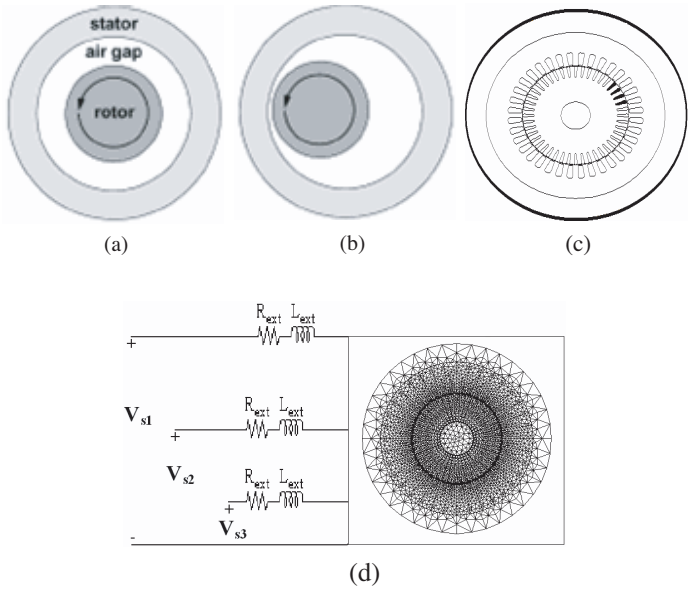

Figure 5. Model of healthy and faulty induction motor.

motor) to the circuit equations is as follows [33].

$$[K \quad C] \begin{bmatrix} A \\ i \end{bmatrix} + [Q \quad R] \begin{bmatrix} \dfrac{\partial \vec{A}}{\partial t} \\ \dfrac{\partial i}{\partial t} \end{bmatrix} = P \tag{1}$$

where $[A]$ and $[i]$ are the magnetic potential vector and any phase stator current that must be determined. $[K]$, $[C]$, $[Q]$ and $[R]$ are the coefficients matrices and P is the vector that related to the input voltage. In the steady-state analysis of induction motor, the on-load and no-load speed must be kept constant. After short time of applying the voltage to the motor, the system reaches the steady-state and then A is determined as follows [33]:

$$[K \quad C] \begin{bmatrix} A \\ I \end{bmatrix} + [Q \quad R] \begin{bmatrix} j\omega A \\ j\omega I \end{bmatrix} = P \tag{2}$$

where ω is the angular frequency which is identical with that of the input voltage. The current vector potential vector A is determined by solving (2).

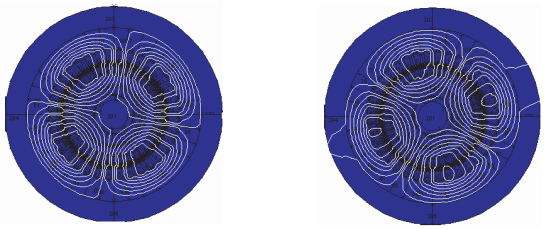

(a) (b)

Figure 6. Magnetic flux distribution for healthy motor and motor with 4 broken bars and 30% eccentricity.

Fig. 6 shows the magnetic flux distribution for healthy motor, a motor with 4 broken rotor bars and 30% eccentricity. Fig. 6(a) presents the magnetic flux distribution of a healthy and symmetrical induction motor.

When the rotor bars are broken, the current of these bars passes the adjacent bars. Lower current of the broken bars means a higher current in its adjacent bars which may saturate those stator and rotor teeth that are close to the adjacent bars. On the other hand, this causes the asymmetrical distribution of the magnetic flux for a motor with static eccentricity. The reason for asymmetry of the magnetic flux distribution is the injection of the harmonics, caused by the static eccentricity fault, to the stator current. The simultaneous faults cause saturation in the stator and rotor teeth close to the broken bar and also degree of asymmetry of the magnetic flux increases. Fig. 6(b) presents the magnetic flux distribution of an induction motor with 4 broken bars and 30% static eccentricity.

The influence of the fault upon the magnetic field distribution of the motor is detected by comparing such distribution for healthy and faulty motors. Influence of different faults on the magnetic vector potential $\vec{A}$ has been shown in Figs. 7–9. The broken rotor bars and static eccentricity (mixed-fault) deviate the magnetic potential vector compared with that of the healthy motor. By rising the degree of eccentricity, this deviation increases, and asymmetrical magnetic field distribution or deviation of the magnetic potential vector results in more harmonic components. This develops vibration torque, asymmetrical magnetic stress, noise and even arc. Taking into account (1) and (2) and determining the magnetic potential vector $\vec{A}$, the magnetic flux density is obtained as follows :

$$\vec{B} = \nabla \times \vec{A} \tag{3}$$

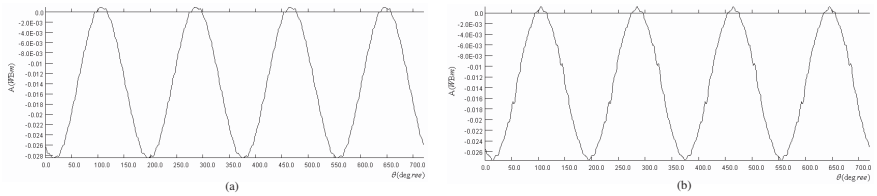

Figure 7. Magnetic vector potential A in the air-gap of healthy induction motor: (a) no-load, (b) full load.

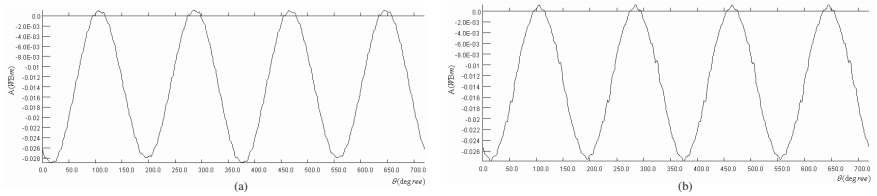

Figure 8. Magnetic vector potential A in the air-gap of induction motor with 1 broken bar and 10% static eccentricity: (a) no-load, (b) full load.

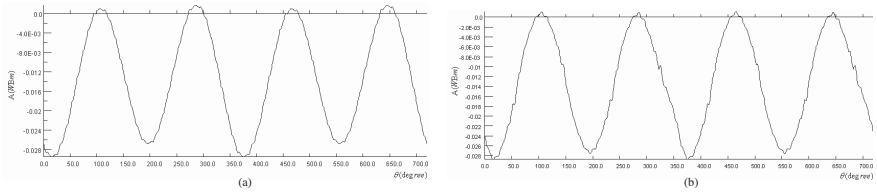

Figure 9. Magnetic vector potential A in the air-gap of induction motor with 4 broken bar and 30% static eccentricity: (a) no-load, (b) full load.

In the normal operation of the motor, the magnetic field within the air gap has the following distribution:

$$B_{normal} = \sum_{n=1,3,5,\ldots} B_n \sin(n\omega t) + \sum_{n=2,4,6,\ldots} B_n \cos(m\omega t) \qquad (4)$$

In (4), the odd harmonics form the main parts of the air-gap MMF waveform and the even harmonics cause the MMF ripples. During the faults, the intensity of the main harmonics and also ripples vary based on the type and degree of the fault. Fig. 10 shows the air gap magnetic flux density distribution for no-load and full-load healthy induction

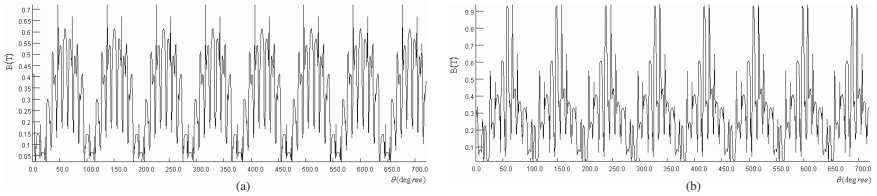

Figure 10. Magnetic flux density B in the air-gap of healthy induction motor: (a) no-load, (b) full load.

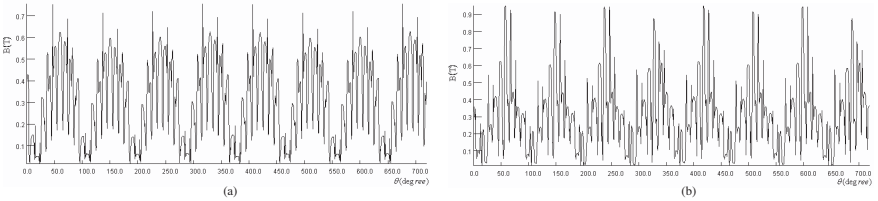

Figure 11. Magnetic flux density B in the air-gap of induction motor with 10% static eccentricity: (a) no-load, (b) full load.

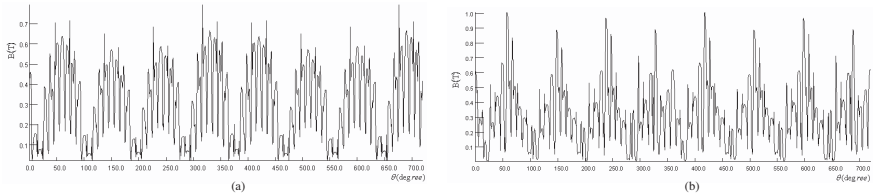

Figure 12. Magnetic flux density B in the air-gap of induction motor with 4 broken bar and 30% static eccentricity: (a) no-load, (b) full load.

motor. Also the influence of different faults on the above-mentioned distributions have been shown in Figs. 11–12.

The fault causes an asymmetry of the magnetic flux density distribution. A higher degree eccentricity fault leads to a more asymmetry of the magnetic flux density distribution. In the case of mixed fault, the air gap field, consisting of the main components, rotor and stator mmf harmonics and the rotor and stator slot permeance harmonics, will results in additional harmonic components due to the fault. Consequently, the main harmonics of the slot in the phase current rises as a function of the asymmetry of the air gap. Therefore, the harmonic components of the stator phase current increase that lead to the rise of the forces variations and electromagnetic torque of the

motor. Since the magnetic forces influence the magnetic field within the motor, the fault and its extension, increases the magnetic force and torque variations rate and consequently it leads to asymmetrical air gap magnetic flux density distribution. This is clear from Figs. 10–12.

4. PERFORMANCE ANALYSIS OF FAULTY INDUCTION MOTOR

In a healthy three-phase motor, the rotating field of the stator and rotor interacts and develops uniform torque. In a faulty motor, there is an opposite field to the stator that induces current in the rotor, and it develops a torque with frequency twice slip frequency which increases the noise and slip. The oscillation frequency of the torque noise rises when the load increases. In the modeling of induction motor using FEM, the schematic figure shown in Fig. 5 is used for electromagnetic torque calculation by Maxwell stress tensor.

Based on the Maxwell stress technique, the stress tensor applied to the rotor surface is as follows:

$$\xi = \frac{B_n^2 - B_t^2}{2\mu_0} \tag{5}$$

where B_n and B_t is the radial and tangential components of the magnetic field respectively. By integrating ξ over the stator and rotor surface, the radial and tangential force and also electromagnetic torque are determined as follows.

$$f_n = \frac{1}{2\mu_0}\left(B_n^2 - B_t^2\right) \tag{6}$$

$$f_t = \frac{1}{\mu_0}\left(B_n B_t\right) \tag{7}$$

$$T_{em} = \frac{r \cdot l}{\mu_0} \oint B_n B_t ds \tag{8}$$

Fig. 13 shows time variations of the electromagnetic torque for healthy motor from the starting up to the steady-state operation, in no-load and full-load cases. Figs. 14–16 show similar curves for different faults. At the starting, the currents of the motor are high, magnetic flux and flux density have very large values. This is especially true for the flux density of the teeth. Ignoring the magnetic saturation in the transient analysis of the induction motor, can reduce the reductances of different sections of the rotor and stator and their teeth. So, the magnetic potential of the teeth is increased considerably. This largely

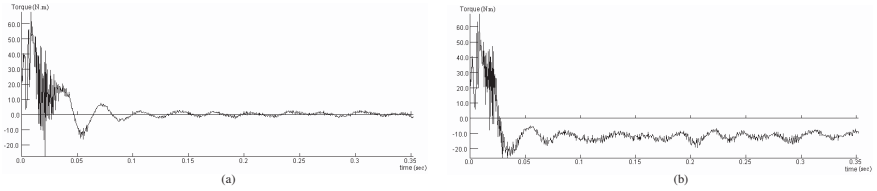

Figure 13. Time variations of torque of a healthy induction motor: (a) no-load, (b) with full load.

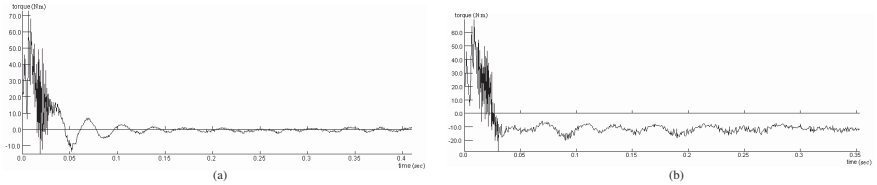

Figure 14. Time variations of torque of a faulty induction motor: with 30% static eccentricity: (a) no-load, (b) full load.

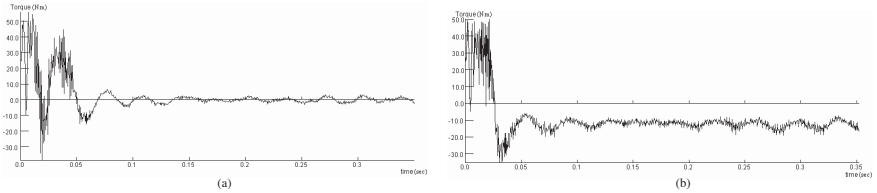

Figure 15. Time variations of torque of a faulty induction motor: with 4 broken bar: (a) no-load, (b) with full load.

increases the rate of the electromagnetic torque variations during the starting period.

Fig. 17 shows time variations of torque for 30% static eccentricity with constant μ. Magnetic saturation decreases the stator self-inductances and also effective magnetizing inductance. Therefore, reluctances of the stator and rotor teeth and thus magnetic potential increase considerably.

Consequently, there is a considerable decrease of the starting electromagnetic torque variations rate compared with that of the constant μ case. Comparison of Figs. 14 and 17 indicates the influence of the saturation upon the analysis of a faulty induction motor.

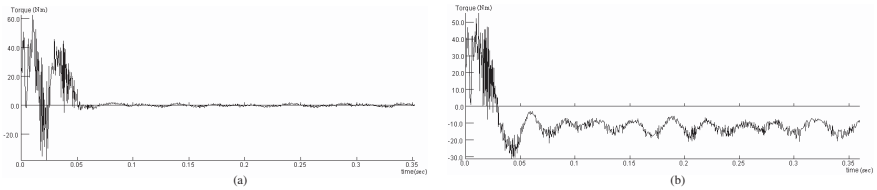

Figure 16. Time variations of torque of a faulty induction motor: with 4 broken bars and 30% static eccentricity: (a) no-load, (b) full load.

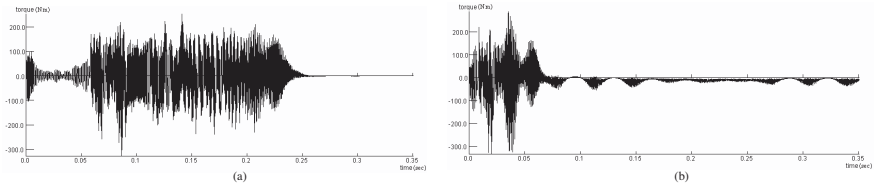

Figure 17. Time variations of torque of a faulty induction motor without magnetization curve with 30% static eccentricity: (a) no-load, (b) full load.

5. CONCLUSION

All faults in electrical motor can be diagnosed accurately using the TSFE technique when the input of the FE computation is the applied voltage. This technique solves the complexities of the FE technique with current-fed, because the terminal voltage of the motor has been considered as the required input value. In addition, it has been found that there is no need to use additional software for some calculations. This prevents the duality in the accuracy during the complete computations process. The mixed fault induction motor has been analyzed which is considered a novel part of the work. Influence of the core saturation upon the analysis of a faulty induction motor has been investigated. In fact steady-state analysis of induction motor does not change that much in the fault case, because the motor operates on the knee of the magnetization characteristic. But in the transient analysis of induction motor, saturation affects the performance of the motor so much due to a very high starting current. It means that the fault diagnosis of induction motor using the transient analysis is not valid if μ is taken to be constant.

REFERENCES

1. Fiser, R., "Application of a finite element method to predict damage induction motor performance," *IEEE Transactions on Magnetic,* Vol. 37, No. 5, 3635–3639, Sep. 2001.
2. Trzynadlosky, A. M., "Diagnostic of mechanical abnormalities in induction motor using instantaneous electrical power," *Proceedings of The 1997 International Electric Machines and Drives Conference,* 91–93, Milwaukee, 1997.
3. Elkasabgy, N. M., A. R. Eastman, and G. E. Dawson, "Detection of broken bars in the cage rotor on an induction machine," *IEEE Transactions on Industry Application,* Vol. IA-22, No. 6, 165–171, 1992.
4. Toliyat, H. A., M. M. Rahimian, S. Bhattacharya, and T. A. Lipo, "Transient analysis of induction machines under internal faults using winding functions," *3rd International Conference on Electrical Rotating Machines-ELROMA,* Bombay, India, 1992.
5. Toliyat, H. A. and T. A. Lipo, "Transient analysis of cage induction machines under stator, rotor bar and end ring faults," *IEEE Trans. Energy Conversion,* Vol. 10, No. 2, 241–247, June 1995.
6. Joksimovic, G. M., M. D. Durovic, J. Penman, and N. Arthur, "Dynamic simulation of dynamic eccentricity in induction machines-winding function approach," *IEEE Trans. Energy Conversion,* Vol. 25, No. 2, 143–149, June 2000.
7. Faiz, J., I. Tabatabaei, and H. A. Toliyat, "An evaluation of inductances of a squirrel-cage induction motor under mixed eccentric conditions," *IEEE Transactions on Energy Conversion,* Vol. 18, No. 2, 252–258.
8. Faiz, J. and I. Tabatabaei, "Extension of winding function theory for non uniform air gap in electric machinery," *IEEE Transactions on Magnetic,* Vol. 38, No. 6, 3654–3657, Nov. 2002.
9. Nandi, S., R. M. Bharadwaj, and H. A. Toliyat, "Performance analysis of a three-phase induction motor under mixed eccentricity condition," *IEEE Transactions on Energy Conversion,* Vol. 17, No. 3, 392–397, Sept. 2002.
10. Nandi, S., S. Ahmed, and H. A. Toliyat, "Detection of rotor slot and other eccentricity related harmonics in a three phase induction motor with different rotor cages," *IEEE Trans. Energy Conversion,* Vol. 16, No. 3, 253–260, Sept. 2001.
11. Ostovcic, V., "A simplified approach to the magnetic equivalent circuit modeling of electric machines," *IEEE Trans. Industrial*

Applications, Vol. IA-24, No. 2, 308–316, Mar. 1988.

12. Lipo, T. A., "The analysis of induction motors with voltage control by symmetrically triggered thyristors," *IEEE Trans. Power Apparatus and Systems,* Vol. PAS-90, No. 2, 515–525, March/April 1971.
13. Smith, J. R., *Response Analysis of AC Machines: Computer Models and Simulation,* Research Studies Press Ltd., Somerset, England, 1990.
14. Barbour, A. and W. T. Thomson, "Finite element study of rotor slot designs with respect to current monitoring for detecting static air-gap eccentricity in squirrel-cage induction motors," *IEEE Industrial Applications Society Annual Meeting,* New Orleans, Louisiana, October 5–8, 1997.
15. Thomson, W. T. and A. Barbour, "An industrial case study of on-line current monitoring and finite element analysis to diagnose air-gap eccentricity problems in large high voltage 3-phase induction motors," *9th International Conference on Electrical Machines and Drives,* Conference Publication No. 468, 1999.
16. Tenhunen, A., T. Bendetti, T. P. Holopainen, and A. Arkkio, "Electromagnetic forces of the cage rotor in conical whirling motion," *IEE Proc. - Electr. Power Apply.,* Vol. 150, No. 5, 563–568, September 2003.
17. Tenhunen, A., T. P. Holopainen, and A. Arkkio, "Effects of saturation on the forces in induction motors with whirling cage rotor," *IEEE Transactions on Magnetics,* Vol. 40, No. 2, 766–769, March 2004.
18. Tenhunen, A., "Calculation of eccentricity harmonics of the air-gap flux density in induction machine by impulse method," *IEEE Transactions on Magnetics,* Vol. 41, No. 5, 1904–1907, May 2005.
19. Pham, T. H., P. F. Wendling, S. J. Salon, and H. Acikgoz, "Transient finite element analysis of an induction motor with external circuit connections and electromechanical coupling," *IEEE Trans. Energy Conversion,* Vol. 14, No. 4, 1407–1412, Dec. 1999.
20. Krefta, M. P. and O. Wasynczuk, "A finite element based state model of solid rotor synchronous machines," *IEEE Transactions Energy Conversion,* Vol. EC-2, No. 1, 21–30, March 1987.
21. Ho, S. C., C. G. Hong, and G. J. Hwang, "Transient and steady state performance of a squirrel-cage induction motor," *IEE Proceedings,* Vol. 136, No. 3, 136–142, May 1989.
22. Williamson, S., L. H. Lim, and A. C. Smith, "Transient analysis

of cage induction motor using finite elements," *IEEE Trans. Magnetics,* Vol. 26, No. 2, 941–944, March 1990.

23. Thorsen, O. V. and M. Dalva, "Failure identification and analysis for high voltage induction motors in petrochemical industry," *IEEE Trans. Ind. A,* Vol. 12, No. 2, 1998.
24. Thomson, W. T., "On line current monitoring and application of a finite element method to predict the level of static air gap eccentricity in three-phase induction motors," *IEEE Transactions on Energy Conversion,* Vol. 13, No. 14, 347–354, Dec. 1998.
25. Demerdash, N. A., J. F. Bangura, and A. A. Arkadan, "A time-stepping coupled finite element-state space model for induction motor drives. I. Model formulation and machine parameter computation," *IEEE Transactions on Energy Conversion,* Vol. 14, No. 4, 1465–1471, Dec. 1999.
26. Bangura, J. F. and N. A. Demerdash, "Effects of broken bars/end-ring connectors and air gap eccentricities on ohmic and core losses of induction motors in ASDs using a coupled finite element-state space method," *IEEE Transactions on Energy Conversion,* Vol. 15, No. 1, 40–47, March 2000.
27. Povinelli, R. J., J. F. Bangura, N. A. O. Demerdash, and R. H. Brown, "Diagnostics of bar and end-ring connector breakage faults in poly phase induction motors through a novel dual track of time-series data mining and time-stepping coupled FE-state space modeling," *Electric Machines and Drives Conference, IEMDC 2001, IEEE International 2001,* 809–813.
28. Povinelli, R. J., J. F. Bangura, N. A. O. Demerdash, and R. H. Brown, "Diagnostics of bar and end-ring connector breakage faults in poly phase induction motors through a novel dual track of time-series Data mining and time-stepping coupled FE-state space modeling," *IEEE Transactions on Energy Conversion,* Vol. 17, No. 1, 39–46, March 2002.
29. Bangura, J. F., R. J. Povinelli, N. A. O. Demerdash, and R. H. Brown, "Diagnostics of eccentricities and bar/end-ring connector breakages in poly phase induction motors through a combination of time series data mining and time-stepping coupled FE-state-space techniques," *Industry Applications, IEEE Transactions on Industry Applications,* Vol. 39, No. 4, 1005–1013, July–Aug. 2003.
30. Toliyat, H. A. and S. Nandi, "Condition monitoring and fault diagnosis of electrical machines — a review," *Proceedings of the IEEE-IAS 1999 Annual Meeting,* 197–204, Phoenix, AZ, Oct. 3–7, 1999.

31. Nandi, S., R. Bharadwaj, H. A. Toliyat, and A. G. Parlos, "Study of three phase induction motors with incipient rotor cage faults under different supply conditions," *Proceedings of the IEEE-IAS 1999 Annual Meeting,* Vol. 3, 1922–1928, 1999.
32. Elkasabgy, N. M., A. R. Eastman, and G. E. Dawson, "Detection of broken bar in the cage rotor on an induction machine," *IEEE Transactions on Industry Application,* Vol. 28, No. 1, January/February 1992.
33. Ho, S. L., W. N. Fu, and H. C. Wong, "An incremental method for studying the steady state performance of induction motors using time stepping finite element model," *IEEE Transactions on Magnetic,* Vol. 33, No. 2, 1374–1377, March 1997.